



Azobenzene-based supramolecular liquid crystals: The role of core fluorination

Mohamed Alaasar^{a,b,*}, Jaques-Christopher Schmidt^b, Ahmed F. Darweesh^a, Carsten Tschierske^b

^a Department of Chemistry, Faculty of Science, Cairo University, Giza, Egypt

^b Institute of Chemistry, Martin Luther University Halle-Wittenberg, Kurt Mothes Str. 2, D-06120 Halle (Saale), Germany

ARTICLE INFO

Article history:

Received 24 March 2020

Received in revised form 23 April 2020

Accepted 28 April 2020

Available online 03 May 2020

Keywords:

Supramolecular liquid crystals

Azobenzene

Hydrogen-bonding

Nematic

Fluorination

Photosensitivity

ABSTRACT

The impact of core fluorination on the phase behaviour of supramolecular hydrogen-bonded liquid crystals (HBLCs) is investigated in detail. Therefore, different types of HBLCs were synthesized using two benzoic acid derivatives as proton donors, namely, 4-octyloxybenzoic acid and octylbenzoic acid. The two acids were combined through intermolecular hydrogen-bonding with alkoxyazopyridine derivatives as proton acceptors. Three different types of azopyridines were used either without fluorine substitution or with one lateral fluorine substituent at different positions. The study proved the importance of using core fluorination as a significant tool to modify the liquid crystalline behaviour of HBLCs, where all azopyridines are non-mesomorphic and almost all their complexes exhibit enantiotropic mesophases. The formation of the hydrogen bond between the complementary components was confirmed using FTIR and ¹H NMR spectroscopy, while the liquid crystalline self-assembly of the HBLCs was investigated in detail using polarized light microscope (PLM) and differential scanning calorimetry (DSC). Depending on the type of the terminal chain on the benzoic acid derivative and on the position of the lateral fluorine substituent different types of mesophases including nematic (N), smectic A (SmA) and smectic C (SmC) phases were observed. Finally, under UV light illumination all the prepared HBLCs show *cis-trans* photoisomerization resulting in tuning the liquid crystalline phases, which is of importance for industrial applications.

© 2020 Elsevier B.V. All rights reserved.

1. Introduction

Liquid crystalline (LC) materials are of special interest for the display technology due to their molecular self-assembly which can be tuned under the effect of external stimuli, temperature or light. Since the first discovery of LC, different classes of molecular structures have been designed to produce several LCs with fascinating properties. A huge number of LCs have been reported using different synthetic methods, however the design of supramolecular liquid crystals by intermolecular interaction between complementary components is of great importance. The intermolecular interactions could be either halogen-bonding [1–6], or hydrogen-bonding [7–9], and both have the advantage of the ease accessibility compared to covalently bonded LCs. Kato et al. reported the first examples of hydrogen bonded liquid crystals (HBLCs) designed by hydrogen-bond formation between pyridine-derivatives and benzoic acid derivatives [10,11] later several HBLCs were designed using different types of proton donors and proton acceptors to produce wide varieties of molecular architectures such as rod-

like HBLCs [12,13], bent-shaped LCs [14–18] polymeric framework [19], modular hierarchical [20], non-symmetric dimers having conventional nematic phases [21] or exhibiting the heliconical twist-bend nematic phase (N_{TB}) [22] and supramolecular polycatenars capable of displaying chiral isotropic liquids beside chiral cubic phases [23]. One class of the commonly used proton acceptors is azopyridine-derivatives [12,13,16,20,21,23–26]. Azopyridines are interesting because they combine the possibility of self-assembly through intermolecular hydrogen- or halogen-bond formation together with the unique phenomenon of *trans-cis* photoisomerization under light irradiation due to the presence of the azo linkage. Azo functionalized LCs are of special interest for the manufacture of light responsive materials for the technological applications such as molecular scissors [27] and photo-oscillators [28,29]. In recent years different types of azobenzene-based LCs with fascinating properties were reported [30–32]. One way to modify the liquid crystalline behaviour is aromatic core fluorination [33–40]. This is caused by the unique combination of high polarity and low polarizability of the fluorine atom, as well as steric and conformational effects. Due to its small size fluorine atom can be accommodated by the molecular core affecting the strength of the electrostatic and π -stacking core-core interactions. In 2003 X. Song et al reported HBLCs between 4-octyloxybenzoic acid and 4-(alkoxyphenylazo) pyridines with

* Corresponding author at: Department of Chemistry, Faculty of Science, Cairo University, Giza, Egypt.

E-mail address: malaasar@sci.cu.edu.eg (M. Alaasar).

Table 1
Phase transition temperatures (T/°C), mesophase types, and transition enthalpies [ΔH (J/g)] of the supramolecular HBLCs **An**, **A3Fn** and **A2Fn**^a.

Complex	n	X	Y	Phase sequence (T/°C [ΔH (J/g)])
A10 [41]	10	H	H	H: Cr 88 [62.2] SmC 128 [22.0] Iso C: Iso 126 [−19.5] SmC 89 [−70.8] Cr
A12 [41]	12	H	H	H: Cr 92 [40.2] SmC 128 [22.0] Iso C: Iso 126 [−19.5] SmC 82 [−43.3] Cr
A14 [41]	14	H	H	H: Cr 90 [82.3] SmC 127 [25.5] Iso C: Iso 126 [−23.5] SmC 82 [−39.3] Cr
A3F8	8	F	H	H: Cr 93 [75.2] N 113 [5.9] Iso C: Iso 111 [−5.3] N 92 [−1.8] SmC 84 [−73.4] Cr
A3F10	10	F	H	H: Cr 84 [46.8] SmC 98 [11.2] ^b N 115 [11.2] ^b Iso C: Iso 110 [−10.0] ^b N 95 [−10.0] ^b SmC 64 [−53.0] Cr
A3F12	12	F	H	H: Cr 87 [59.7] SmC 111 [16.2] ^b N 116 [16.2] ^b Iso C: Iso 114 [−14.8] ^b N 108 [−14.8] ^b SmC 73 [60.6] Cr
A3F14	14	F	H	H: Cr 88 [73.6] SmC 115 [18.9] Iso C: Iso 111 [−17.6] SmC 73 [−73.5] Cr
A2F8	8	H	F	H: Cr 96 [51.2] SmC 107 [3.6] N 116 [0.3] Iso C: Iso 110 [−0.2] N 105 [−2.1] SmC 88 [−50.6] Cr
A2F10	10	H	F	H: Cr 86 [80.5] SmC 102 [2.0] N 113 [5.3] Iso C: Iso 111 [−5.5] N 100 [−1.8] SmC 79 [−47.6] Cr
A2F12	12	H	F	H: Cr 93 [85.6] SmC 108 [16.4] ^b N 114 [16.4] ^b Iso C: Iso 110 [−14.4] ^b N 106 [−14.4] ^b SmC 79 [−49.8] Cr
A2F14	14	H	F	H: Cr 85 [66.7] SmC 110 [18.2] Iso C: Iso 108 [−15.4] SmC 75 [−48.5] Cr

^a Peak temperatures as determined from 2nd heating (**H**) and 2nd cooling (**C**) DSC scans with rate 10 K min^{−1}; abbreviations: Cr = crystalline solid; SmC = smectic C phase; SmA = smectic A phase; N = nematic phase; Cr = crystalline solid; Iso = isotropic liquid.

^b The enthalpy value of Iso-N phase transition could not be separated from that of the N-SmC phase transition (see Fig. S5 in the SI).

variable chain lengths (the supramolecules **A10–A14** in Table 1) [41] and it was found that all of **An** complexes exhibit smectic C (SmC) phases regardless the alkoxy chain lengths in the proton acceptor. It was interesting for us to check how lateral fluorine substitution could affect the liquid crystalline behaviour of **An** complexes. To answer this question, we prepared different types of azopyridine derivatives without any fluorine substitution (**Hn**) [23] or with one fluorine substituent either at ortho position with respect to the terminal alkoxy chain (**3Fn**) [42] or at meta position with respect to the terminal alkoxy chain (**2Fn**) (see Scheme 1). All of the synthesized azopyridine derivatives (**Hn**, **3Fn** and **2Fn**) were found to be non-mesomorphic and were used as proton acceptors to prepare new fluorinated HBLCs by intermolecular H-bond formation with the mesomorphic 4-octyloxybenzoic acid (**A3Fn** and

A2Fn) to compare it with the previously reported **An** complexes. Moreover, the effect of removing the oxygen atom connecting the terminal chain on the benzoic acid on the LC behaviour of the synthesized HBLCs was investigated systemically by preparing other types of H-bonded aggregates (**Bn**, **B3Fn** and **B2Fn**) using the nematogenic 4-octylbenzoic acid as the proton donor instead of 4-octyloxybenzoic acid.

2. Experimental

2.1. Synthesis

The synthesis of the HBLCs is shown in Scheme 1. The benzoic acid derivatives are commercially available, while the azopyridine

Table 2
Phase transition temperatures (T/°C), mesophase types, and transition enthalpies [ΔH (J/g)] of the supramolecular HBLCs **Bn**, **B3Fn** and **B2Fn**^a.

Complex	n	X	Y	Phase sequence (T/°C [ΔH (J/g)])
B8	8	H	H	H: Cr 100 [48.5] SmA 124 [23.7] Iso C: Iso 121 [−23.4] SmA 88 [−47.4] Cr
B10	10	H	H	H: Cr 89 [35.7] SmC 105 [−] SmA 123 [24.8] Iso C: Iso 119 [−23.6] SmA 104 [−] SmC 77 [−34.9] Cr
B12	12	H	H	H: Cr 90 [33.4] SmC 119 [−] SmA 124 [27.6] Iso C: Iso 121 [−25.8] SmA 115 [−] SmC 81 [−16.6] Cr
B14	14	H	H	H: Cr 88 [30.7] SmC 122 [−] SmA 124 [28.1] Iso C: Iso 121 [−28.8] SmA 119 [−] SmC 89 [−8.4] SmX 79 [−13.3] Cr
B3F8	8	F	H	H: Cr 88 [47] SmC 102 [11.7] Iso C: Iso 99 [−11.7] SmC 71 [−43.6] Cr
B3F10	10	F	H	H: Cr 87 [53.2] SmC 101 [9.5] Iso C: Iso 96 [−10.9] SmC 72 [−55.3] Cr
B3F12	12	F	H	H: Cr 83 [49.2] SmC 106 [16.3] Iso C: Iso 102 [−14.9] SmC 68 [−52.2] Cr
B3F14	14	F	H	H: Cr 89 [64.1] SmC 106 [19.4] Iso C: Iso 103 [−18.0] SmC 74 [−63.8] Cr
B2F8	8	H	F	H: Cr 94 [53.4] Iso C: Iso 94 [−7.7] SmA 80 [−36.1] Cr
B2F10	10	H	F	H: Cr 90 [42.0] SmA 106 [19.6] Iso C: Iso 102 [−17.5] SmA 72 [−45.3] Cr
B2F12	12	H	F	H: Cr 84 [45.7] SmC 93 [−] SmA 108 [22.8] Iso C: Iso 105 [−21.6] SmA 92 SmC [−] 70 [−41.5] Cr
B2F14	14	H	F	H: Cr 83 [43.0] 95 SmC [−] SmA 108 [19.1] Iso C: Iso 104 [−20.6] SmA 94 SmC [−] 68 [−37.9] Cr

^a Peak temperatures as determined from 2nd heating (**H**) and 2nd cooling (**C**) DSC scans with rate 10 K min^{−1}; abbreviations: SmA = smectic A phase; SmX = unidentified smectic phase. For other abbreviations see Table 1.

derivatives with or without fluorine substitution were synthesized as described in the supporting information (SI) by a coupling reaction between the diazonium salt of 4-aminopyridine and phenol, 2-fluorophenol or 3-fluorophenol followed by etherification of the resulting azo dyes with different alkyl bromides to give the target proton acceptors. The analytical data for 4-(3-fluoro-4-dodecyloxyphenylazo)pyridine **3F12** and 4-(2-fluoro-4-dodecyloxyphenylazo)pyridine **2F12** are given below as representative examples. The supramolecular HBLCs (**An**, **A3Fn**, **A2Fn**, **Bn**, **B3Fn** and **B2Fn**) were prepared by mixing equimolar amounts of each of the azopyridine derivatives (**Hn**, **3Fn** or **2Fn**) and each of the benzoic acid derivatives (**OC8** or **C8**) and melting them together in a DSC pan with stirring to give an intimate blend then cooling to room temperature. The obtained crystals were then melted, and the process was repeated two additional times. Homogenous melting and reproducible phase transition temperatures were observed for all complexes (Table 1).

2.1.1. 4-(3-Fluoro-4-dodecyloxyphenylazo)pyridine, **3F12**

Orange crystals. Melting point: 66 °C, 0.58 g, 68% yield. $^1\text{H NMR}$ (500 MHz, CDCl_3) δ 8.86–8.68 (m, 2H, Ar–H), 7.82 (ddd, $J = 8.7, 2.4, 1.3$ Hz, 1H, Ar–H), 7.72 (dd, $J = 11.9, 2.3$ Hz, 1H, Ar–H), 7.69–7.63 (m, 2H, Ar–H), 7.09 (t, $J = 8.6$ Hz, 1H, Ar–H), 4.14 (t, $J = 6.6$ Hz, 2H, O–CH₂), 2.07–1.70 (m, 2H, O–CH₂–CH₂), 1.55–1.15 (m, 18H, CH₂), 0.88 (t, $J = 6.9$ Hz, 3H, CH₃). $^{13}\text{C NMR}$ (126 MHz, CDCl_3) δ 157.07, 153.86, 151.88, 151.30, 151.24, 151.15, 146.23 (d, $J = 5.6$ Hz), 124.28 (d, $J = 2.9$ Hz), 116.15, 113.39 (d, $J = 2.3$ Hz), 107.89 (d, $J = 19.5$ Hz), 69.57, 31.89, 29.63, 29.55, 29.51, 29.32, 29.30, 29.01, 25.86, 22.66, 14.09. $^{19}\text{F NMR}$ (470 MHz, CDCl_3) δ –132.38 (dd, $J = 11.9, 8.4$ Hz). **MS (ESI)**: m/z (%): positive: 408.2421 ($[\text{M} + \text{Na}]^+$, $\text{C}_{23}\text{H}_{32}\text{FN}_3\text{O} + \text{Na}^+$, calc.: $m/z = 408.24$).

2.1.2. 4-(2-Fluoro-4-dodecyloxyphenylazo)pyridine, **2F12**

Orange crystals. Melting point: 67 °C, 0.50 g, 56% yield. $^1\text{H NMR}$ (500 MHz, CDCl_3) δ 8.91–8.61 (m, 2H, Ar–H), 7.81 (m, 1H, Ar–H), 7.71–7.62 (m, 2H, Ar–H), 6.88–6.62 (m, 2H, Ar–H), 4.04 (t, $J =$

6.5 Hz, 2H, O–CH₂), 1.82 (m, 2H, O–CH₂CH₂), 1.51–1.42 (m, 2H, CH₂), 1.41–1.21 (m, 16H, CH₂), 1.05–0.73 (m, 3H, CH₃). $^{13}\text{C NMR}$ (126 MHz, CDCl_3) δ 164.46, 164.37, 163.37, 161.30, 157.47, 151.27, 134.74 (d, $J = 7.0$ Hz), 118.66, 116.22, 111.61 (d, $J = 2.7$ Hz), 102.33 (d, $J = 23.3$ Hz), 68.98, 31.89, 29.63, 29.61, 29.55, 29.51, 29.32, 29.29, 28.95, 25.90, 22.66, 14.09. $^{19}\text{F NMR}$ (470 MHz, CDCl_3) δ –116.75 to –121.48 (m). **MS (ESI)**: m/z (%): positive: 408.2422 ($[\text{M} + \text{Na}]^+$, $\text{C}_{23}\text{H}_{32}\text{FN}_3\text{O} + \text{Na}^+$, calc.: $m/z = 408.24$).

3. Characterization

Thin layer chromatography (TLC) was performed on aluminium sheet precoated with silica gel. Analytical quality chemicals were obtained from commercial sources and used as obtained. The solvents were dried using the standard methods when required. The purity and the chemical structures of all synthesized materials were confirmed by the spectral data. The structure characterization of the prepared materials is based on $^1\text{H NMR}$, $^{13}\text{C NMR}$, $^{19}\text{F NMR}$ (Varian Unity 400 spectrometers, in CDCl_3 solution, with tetramethylsilane as internal standard) and high resolution mass spectroscopy.

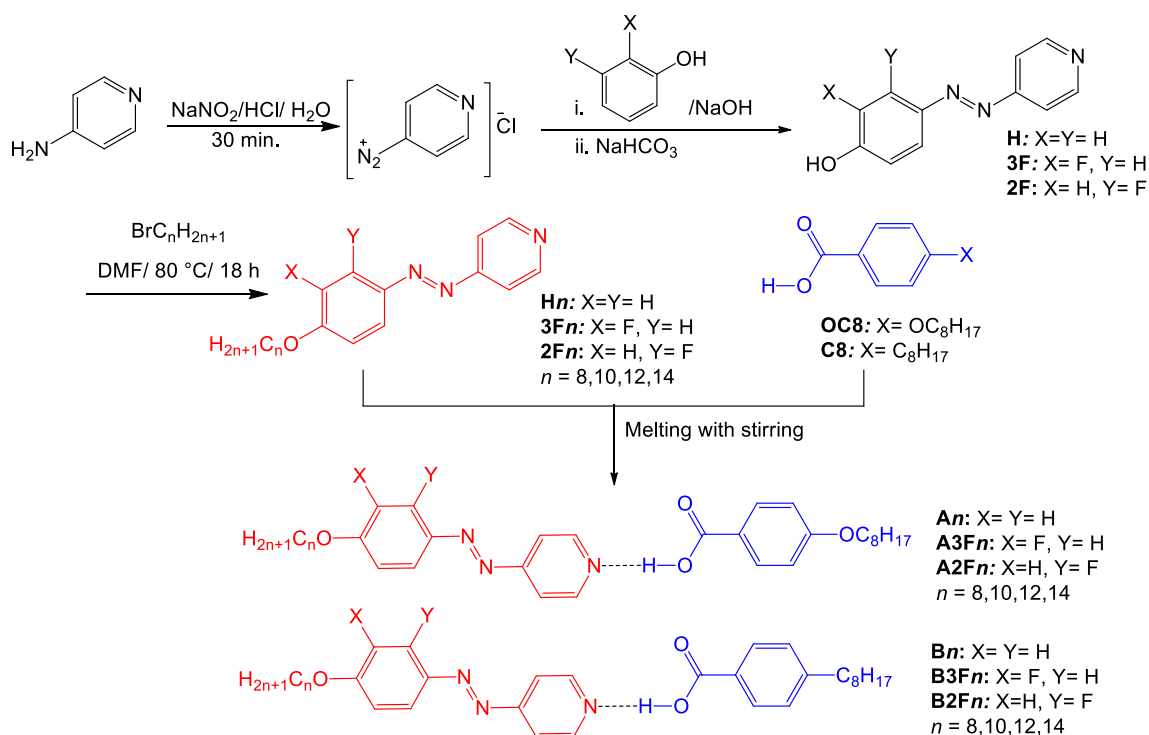
Infrared absorption spectra were measured in dry KBr with a Perkin-Elmer B25 spectrophotometer.

The mesophase behaviour and transition temperatures of the supramolecular complexes were measured using a Mettler FP-82 HT hot stage and control unit in conjunction with a Nikon Optiphot-2 polarizing microscope. The associated enthalpies were obtained from DSC-thermograms which were recorded on a Perkin-Elmer DSC-7, heating and cooling rate: 10 K min⁻¹.

4. Results and discussion

4.1. FTIR and NMR measurements

As an effective tool to investigate the intermolecular interactions [43,44,16], FTIR spectroscopy was performed for the supramolecule



Scheme 1. Synthesis of the azopyridines (**Hn**, **3Fn** and **2Fn** and **23F8**) and the hydrogen-bonded supramolecules (**An**, **A3Fn**, **A2Fn**, **Bn**, **B3Fn** and **B2Fn**).

B2F14 as a representative example for the prepared HBLCs in crystalline state (KBr) at room temperature to prove the formation of the hydrogen-bond between the benzoic acid derivatives and the azopyridines. Fig. 1a, b shows the IR spectra of **B2F14** and its complementary components the azopyridine derivative **2F14** and the proton donor **C8** at two different regions (see Figs. S1–S3 in the SI for the complete range of spectra).

The absence of a band at around 3000 cm^{-1} together with the appearance of two bands at around 2479 cm^{-1} and 1888 cm^{-1} (black curve in Fig. 1a) clearly indicate the formation of 1:1 hydrogen-bonded complex between the azopyridine derivative **2F14** and the benzoic acid **C8** [26,31]. Moreover, the carbonyl stretching vibration band of the pure benzoic acid **C8** which is present in a dimeric form as a result of the intermolecular hydrogen-bond formation between the free carboxylic groups is observed at around 1680 cm^{-1} (blue curve in Fig. 1b) and upon complexation with the proton acceptor **2F14** it is shifted to higher value $\sim 1693\text{ cm}^{-1}$ (i.e. blue shifted, black curve in Fig. 1b). This indicates the formation of another intermolecular hydrogen bond between the monomeric form of **C8** and the pyridine based derivative **2F14** which also confirms the formation of the supramolecule **B2F14** [26,31,45].

Whereas IR confirms complex formation in the solid state, ^1H NMR spectroscopy was used to prove the hydrogen-bond formation in solution. Fig. 2 shows the ^1H NMR spectroscopy in the aromatic region of the supramolecule **A3F14** and its complementary components the proton donor **OC8** and the proton acceptor **3F14** as representative examples (See Fig. S4 for the complete ^1H NMR spectra).

The spectra of the proton acceptor **3F14** shows that the signal corresponding to the hydrogen atoms at ortho positions to the nitrogen atom in the pyridine ring appears at δ 8.86–8.68 ppm (red curve in Fig. 2) and upon hydrogen bond formation it becomes broad and shifted to δ 8.89–8.74 ppm (black curve in Fig. 2). Also, the signal appearing at δ 7.68 ppm in the pure azopyridine-based component **3F14** which corresponds to the protons at meta positions to the nitrogen atom in the pyridine ring is slightly low field shifted and overlaps with the hydrogens at the fluorinated ring after complexation and become more closer to each other's (compare the red and black curves in Fig. 2).

4.2. Liquid crystalline behaviour of **An**, **A3Fn** and **A2Fn**

The phase transition temperatures and types of LC phases of the prepared HBLCs are revealed based on DSC measurements and textural observations under PLM. The obtained data for **An**, **A3Fn** and **A2Fn** are summarized in Table 1 and represented graphically on Fig. 3a–c, while those of **Bn**, **B3Fn** and **B2Fn** are collected in Table 2 and plotted on Fig. 3d–f. As representative examples the DSC traces of **A3F14** and **B14** are shown in Fig. 4.

The benzoic acid derivative used to prepare the first type of the HBLCs i.e. 4-octyloxybenzoic acid forms smectic C (SmC) and nematic (N) phases in the following sequence: Cr 101°C SmC 107°C N 147°C Iso, while all of the individual azopyridine derivatives are nonmesomorphic and melts directly to isotropic liquids (see Table S1 in the SI). As can be seen from Table 1 the nonfluorinated HBLCs (**An**) exhibit only SmC phases as enantiotropic mesophases and the nematic phase is not observed for any of **An** derivatives [41].

The HBLCs **A3Fn** having a fluorine atom at ortho position next to the terminal chain at the azopyridine derivatives show different phase behaviour (Fig. 3b). For the shortest complex **A3F8** an enantiotropic LC phase is observed over $\sim 20\text{ K}$, which show typical observation of the conventional nematic phase (N) with a characteristic schlieren texture containing two- and four-point brush singularities in untreated cells (Fig. 5a). On cooling **A3F8** from the isotropic liquid the nematic phase is observed followed by a monotropic SmC phase (Fig. 5b). This transition is accompanied by an enthalpy transition value in the DSC cooling curve of **A3F8** indicating a first order transition (Table 1). On chain elongation and for the next homologue (**A3F10**) the SmC phase becomes an

enantiotropic LC phase with wider range compared to that observed for **A3F8** and on further chain elongation the range of the SmC phase becomes more wider on the expense of the nematic phase. For the supramolecules with $n = 10$ and 12 the transition enthalpy values for the SmC–N and N–Iso transitions on heating and cooling scans cannot be separated from each other's (see Table 1 and Fig. S5 in the SI). For the longest complex **A3F14** the nematic phase is totally removed and the SmC phase is the only observed mesophase. The range of the SmC phase of **A14** is wider than that of the fluorinated supramolecules **A3Fn**. This also applies for all **An** complexes compared to **A3Fn** irrespective of the terminal chain length on the azopyridine segment.

Changing the position of the lateral fluorine atom from ortho position with respect to the terminal chain on the proton acceptors i.e. the azopyridine derivatives to be at meta position leads to the **A2Fn** complexes. The phase behaviour of **A2Fn** complexes is very similar to that of **A3Fn** complexes (Fig. 5c and Fig. S6 in the SI), however the SmC phase is more stabilized and is observed as enantiotropic phase starting from the shortest homologue **A2F8**.

4.3. Liquid crystalline behaviour of **Bn**, **B3Fn** and **B2Fn**

In order to investigate the effect of removing the oxygen atom connecting the terminal octyl chain to the benzoic acid on the

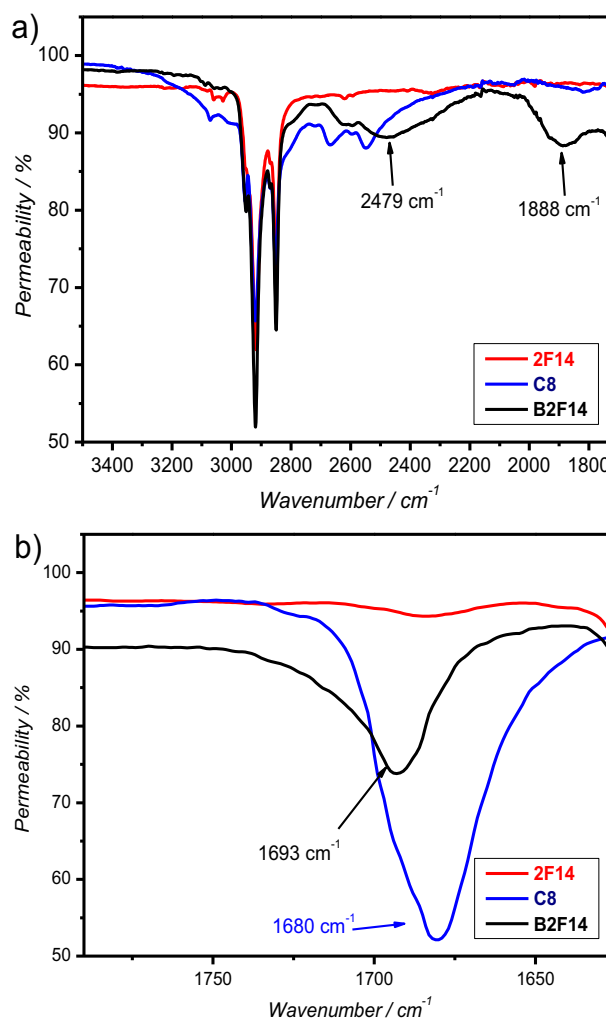


Fig. 1. FTIR spectra of the supramolecule **B2F14** (black) and its complementary components **C8** (blue) and **2F12** (red) in the crystalline state (KBr) at room temperature: a) enlarged area between 1700 cm^{-1} and 3500 cm^{-1} ; b) enlarged area between 1630 cm^{-1} and 1790 cm^{-1} . (For interpretation of the references to colour in this figure legend, the reader is referred to the web version of this article.)

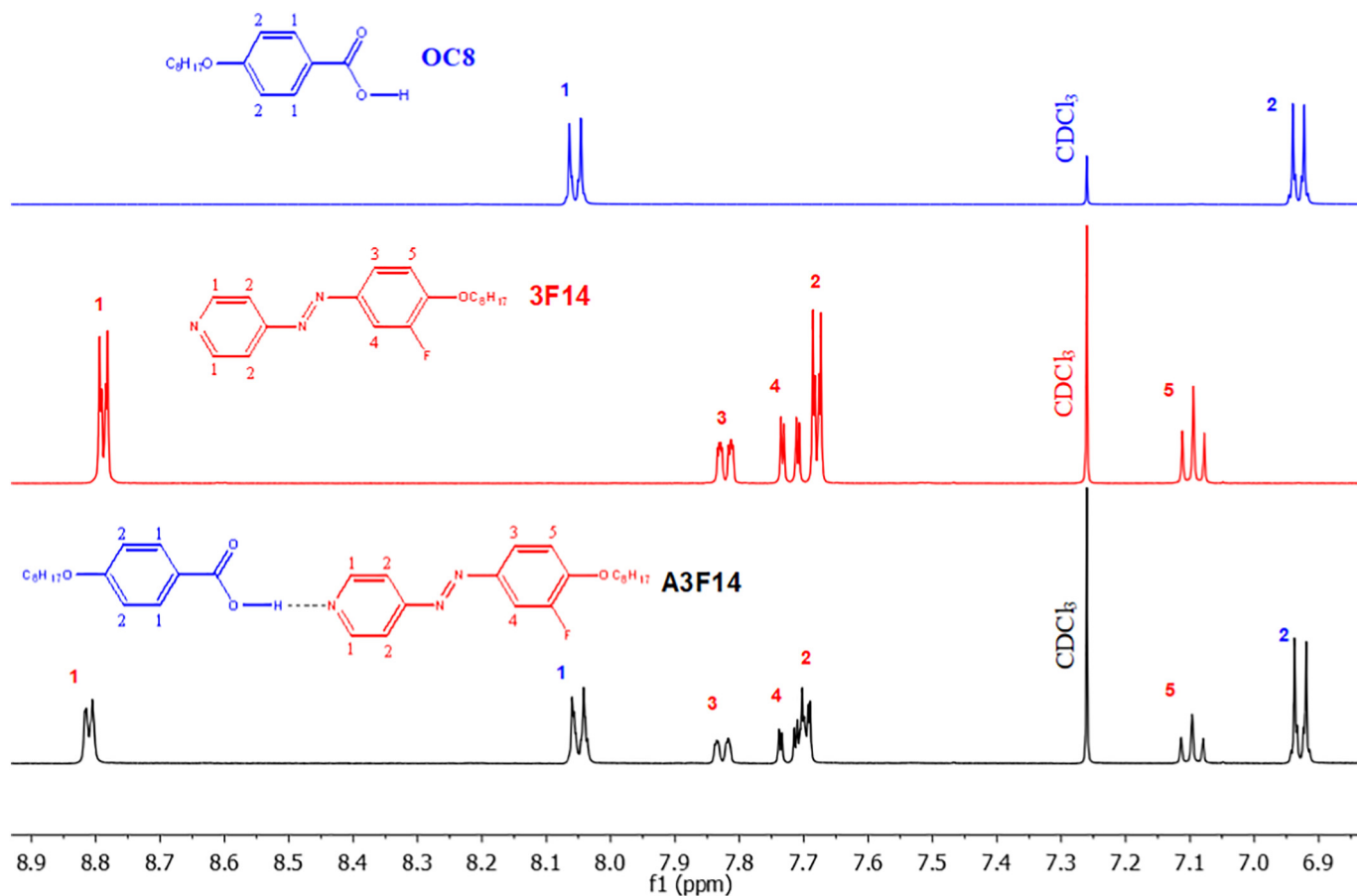


Fig. 2. ^1H NMR spectra (500 MHz, CDCl_3) in the aromatic region of the supramolecule **A3F14** (black) and its complementary components **OCS** (blue) and **3F14** (red). The blue numbers are for the benzoic acid **OCS** protons and the red numbers are for the azopyridine **3F14** protons before and after complexation. (For interpretation of the references to colour in this figure legend, the reader is referred to the web version of this article.)

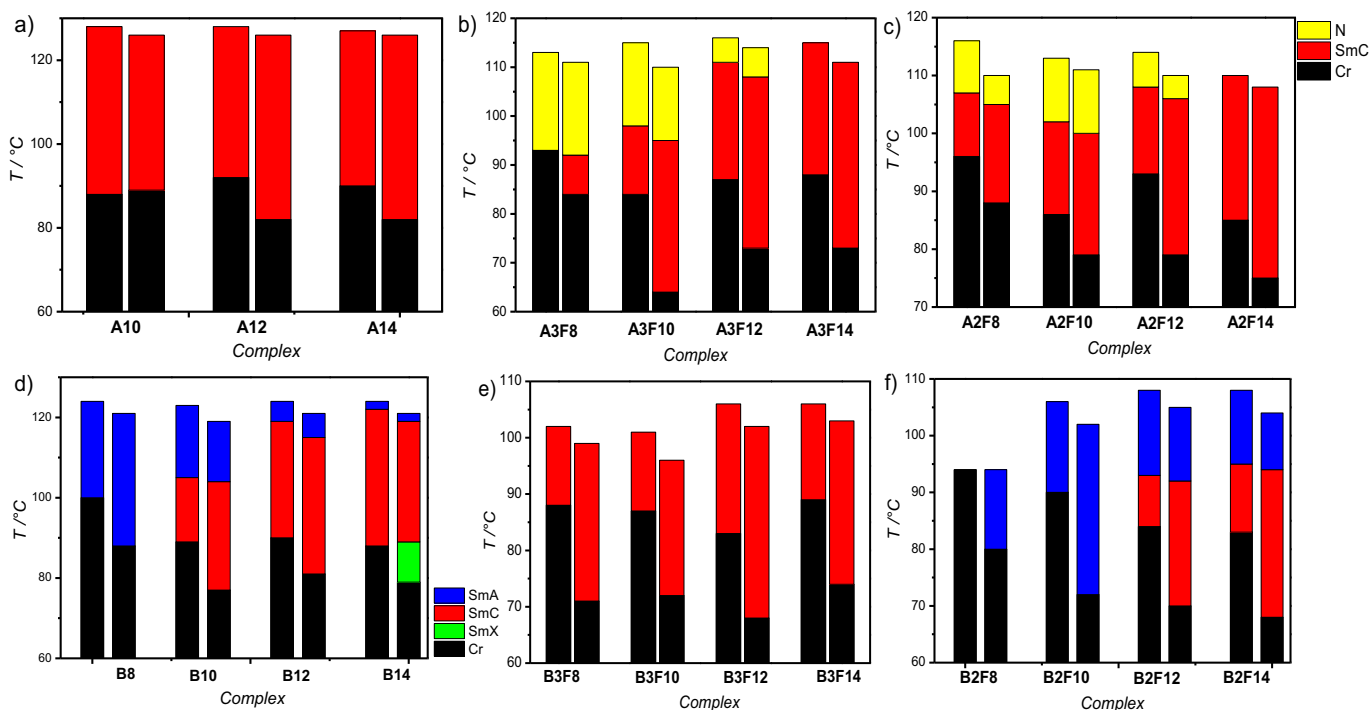


Fig. 3. Phase diagrams of the supramolecular HBLCs: a) **A1n** [41], b) **A3Fn**, c) **A2Fn**, d) **Bn**, e) **B3Fn** and f) **B2Fn**. The phase types are shown in c) and d).

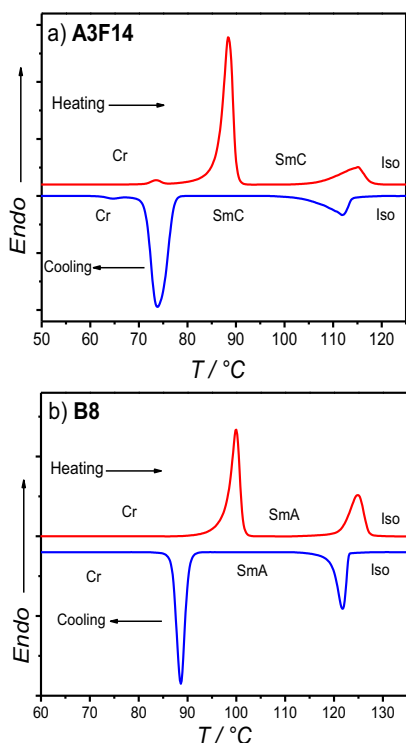


Fig. 4. DSC traces of a) **A3F14** and b) **B8** with heating and cooling rates 10 K/min.

mesophase behaviour of the HBLCs **An**, **A3Fn** and **A2Fn** we prepared another related H-bonded complexes (**Bn**, **B3Fn** and **B2Fn**) using 4-octylbenzoic acid as the proton donor instead of 4-octyloxybenzoic acid. The results prove that this slight modification has a great effect on the liquid crystalline behaviour of the HBLCs. The pure 4-octylbenzoic acid (**C8**) exhibits only a nematic phase in the following sequence: Cr 100 °C N 109 °C Iso, while all of the HBLCs do not exhibit N phases and form different types of mesophases.

As can be seen from Table 2 and Fig. 3d–f the nonfluorinated HBLCs (**Bn**) exhibit three different types of mesophases depending on the chain length and temperatures. For the shortest homologue **B8** only SmA phase is observed based on the textural observations (see Fig. 6 as an example), where totally isotropic texture is observed on the homeotropic cell and a truncated focal conic fan texture is observed in the planar cell confirming the presence of a SmA phase. For the next longer homologues **B10–B14** (with $n \geq 10$) SmC phase starts to appear below the SmA phase as indicated from the DSC traces (Table 1) and the change in the optical textures under the PLM. The range of the SmC phase increases with chain elongation, while that of the SmA phase is suppressed (see Fig. 3d).

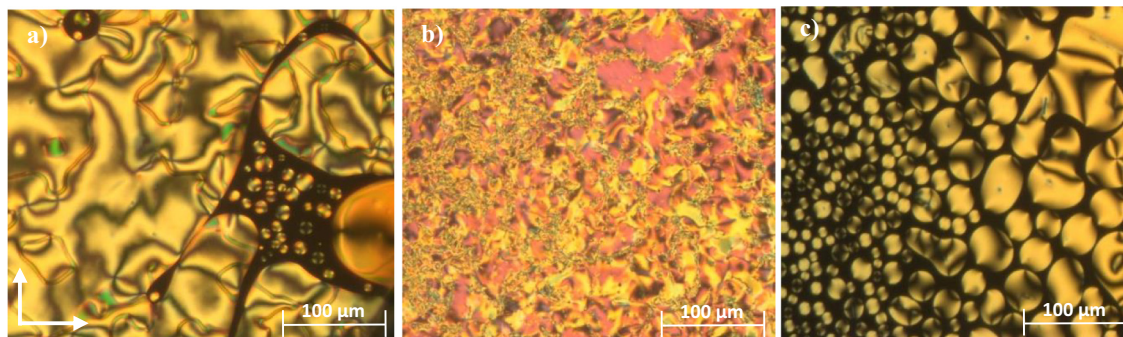


Fig. 5. Photomicrographs of: **A3F8** in a) the N phase at 108 °C and in b) the SmC phase at 89 °C and c) **A2F10** in the N phase at 110 °C. The direction of the polarizers is shown in a).

As shown in Fig. 6a, b at the transition to the SmC phase from the SmA phase the birefringence in the homeotropic cell suddenly increases indicating the tilt of the molecules, while in the planar cell the fan shaped textures become broken as typically observed for SmC phases. The orientation of the extinctions becomes inclined with the directions of polarizer and analyzer indicating a synclinc SmC phase. On further cooling **B14** from the SmC phase the birefringence changes again at ~ 89 °C on both homeotropic and planar cells indicating the transition to another LC phase (Fig. 6c, f). The formation of this phase is associated with a large enthalpy change ~ 8.4 J/g (Table 2), indicating the formation of additional monotropic highly ordered unidentified smectic LC phase assigned as SmX phase below the SmC phase for the longest homologue. As the inclination of the extinctions is retained a transition to a tilted low temperature hexatic (HexI) or crystalline mesophases (CrI/G) is likely. The schlieren texture in Fig. 6c is in favour for a HexI phase, whereas the CrI/G phases are known to prefer moasic like textures [46].

Using 4-(3-fluoro-4-alkoxyphenylazo)pyridines (**3Fn**) as proton donors leads to **B3Fn** HBLCs having a fluorine substituent at ortho position with respect to the terminal alkoxy chain at the azopyridine side. All derivatives of **B3Fn** complexes show only enantiotropic SmC mesophases with comparable melting and clearing temperatures. Changing the position of the fluorine atom to be in meta position leads to the formation of **B2Fn** complexes. The shortest complex **B2F8** melts directly to the isotropic liquid on heating from the crystalline solid and on cooling it exhibits short range of the SmA phase. The SmA phase converts to an enantiotropic phase for all next longer homologues (with $n \geq 10$) which appears as the only mesophase for the complex **B2F10** and beside SmC phases for **B2F12** and **B2F14**.

The results obtained for the prepared supramolecular aggregates indicate that for both types of complexes **An** or **Bn** without fluorine substitution core fluorination leads to lower clearing temperatures (Fig. 3) i.e. lower mesophase stability. However, the type of the mesophases exhibited by HBLCs could be modified by fluorination. Therefore, for the fluorinated complexes **A3Fn** and **A2Fn** nematic and SmC phases were observed, while the nonfluorinated supramolecules **An** exhibit only SmC phases. The same effect was also observed for the other types of the complexes **Bn**, **B3Fn** and **B2Fn**, where the SmA phases are exhibited by the HBLCs or suppressed depending on the position of the fluorine substitution (Fig. 3d–f).

5. Photosensitivity

The prepared supramolecular complexes were designed to be photosensitive due to the presence of the azopyridine segments in its molecular structures. We found that all of the prepared HBLCs are photosensitive and undergo a fast and reversible isothermal phase transition upon illumination with a UV laser pointer (405 nm, 5 mW/mm²). This is due to the *trans-cis* photoisomerization of the azo unit upon photo illumination. The photosensitivity of the supramolecule **B10** will be discussed here in details as a representative example (see Fig. S7 in

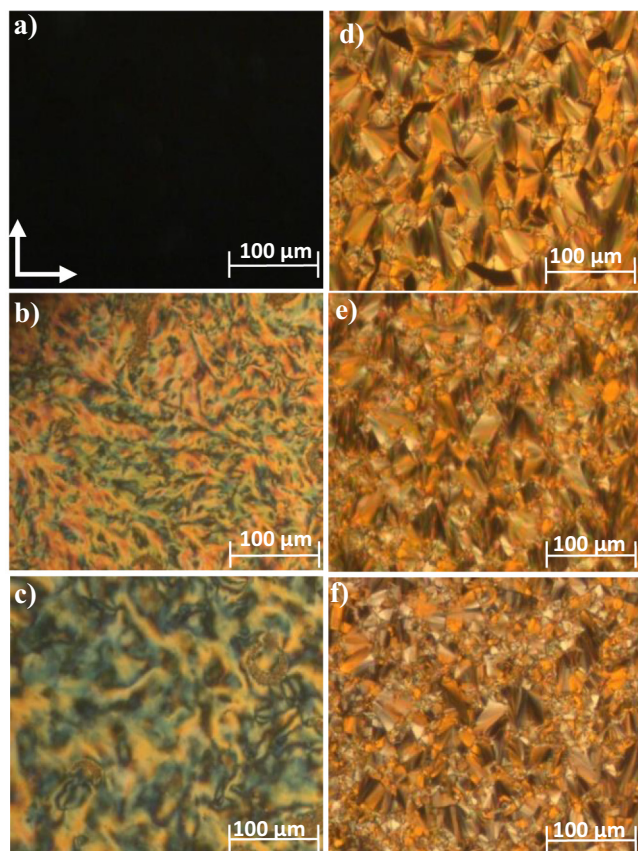


Fig. 6. Optical textures of the supramolecular complex **B14** a–c) in homeotropic cell and d–f) in 10 μm ITO coated cell: a, d) in SmA phase at 120 $^{\circ}\text{C}$; b), e) in SmC phase at 95 $^{\circ}\text{C}$ and c, f) in the SmX phase at 88 $^{\circ}\text{C}$. The direction of the polarizers is shown in a).

the SI for UV–Vis spectroscopy in solution). **B10** exhibits enantiotropic SmC and SmA phases, therefore we investigated the photoinduced SmC–SmA and SmA–Iso phase transitions in homeotropic cells. The SmC phase has a birefringent homeotropic texture under crossed polarizers prior to the UV illumination (Fig. 7a). Under UV irradiation and at 5 K below the SmC–SmA transition temperature i.e. $\sim 99^{\circ}\text{C}$ the birefringent textures disappeared and converts within 3 s into the totally dark homeotropic texture of the uniaxial SmA phase (Fig. 7b). On removing the UV source, the dark texture relaxes back to the original SmC texture in few seconds, indicating a fast and reversible photoinduced phase transition between the SmC and SmA phases. Similar photoinduced phase transition was also achieved between the SmA phase

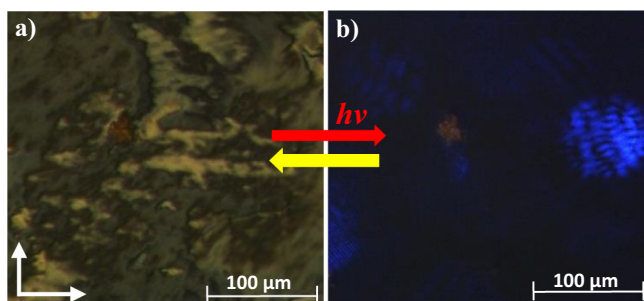


Fig. 7. Textures of the supramolecular complex **B10** under crossed polarizers: a) in the homeotropic aligned SmC phase at $T = 99^{\circ}\text{C}$ before UV irradiation and b) after UV irradiation indicating the transformation from the biaxial SmC phase to the uniaxial SmA phase. The blue colour in b) is due to the UV light. (For interpretation of the references to colour in this figure legend, the reader is referred to the web version of this article.)

and the isotropic liquid phase. Therefore, the SmC–SmA or SmA–Iso transitions achieved upon UV irradiation both resulting from *trans*–*cis* photoisomerization between the more stable *trans* form of the azopyridines before light irradiation and the less stable *cis* form after irradiation [4].

6. Summary and conclusions

In summary, we have reported herein the design and synthesis of new azopyridine derivatives which have been used to prepare new photosensitive supramolecular liquid crystals via intermolecular hydrogen bond formation with two different types of benzoic acid derivatives. The formation of the supramolecular HBLCs was confirmed by FTIR, ^1H NMR, DSC and PLM. Where all the azopyridine derivatives are crystalline solids, all their H-bonded aggregates exhibit LCs phases. They show rich mesomorphism depending on the position of the lateral fluorine substituent, on the terminal chain length and on the type of the proton donor. The supramolecules derived from 4-octyloxybenzoic acid and non-fluorinated azopyridines exhibit only SmC phases irrespective of the terminal chain length (**An** complexes). Using fluorine substituted azopyridines either at ortho or meta positions with respect to the terminal chains as the proton acceptors with 4-octyloxybenzoic acid (**A3Fn** and **A2Fn** complexes) results in additional nematic phases beside the SmC phases for short and medium chains supramolecules (with $n = 8$ –12). Removing the oxygen atom connecting the terminal octyl chain to the benzoic acid results in the related HBLCs **Bn**, **B3Fn** and **B2Fn** constructed using 4-octylbenzoic acid as the proton donor instead of 4-octyloxybenzoic acid. The later complexes do not exhibit nematic phases but form SmA, SmC phases, and in one case of a non-fluorinated complex an additional unidentified low temperature smectic phase assigned as SmX. The effect of changing the position of the lateral fluorine substituent was found to be more pronounced in these types of complexes, where ortho fluorinated complexes (**B3Fn**) exhibit SmC phases and their related meta fluorinated complexes (**B2Fn**) exhibit SmA and SmC phases. Moreover, all of the prepared complexes show fast and reversible photoinduced LCs phase transitions under UV irradiation due to *trans*–*cis* photoisomerization of the azopyridine units. Therefore, the transition between different types of LCs phases or between the LCs phases and the isotropic liquid could be affected with UV light, which provide additional possibility of phase modulation by interaction with light.

CRedit authorship contribution statement

Mohamed Alaasar: Conceptualization, Supervision, Writing - original draft, Writing - review & editing. **Jaques-Christopher Schmidt:** Investigation. **Ahmed F. Darweesh:** Investigation. **Carsten Tschierske:** Writing - review & editing.

Declaration of competing interest

The authors declare no conflict of interest.

Acknowledgements

Ahmed F. Darweesh acknowledges the support by the Alexander von Humboldt Foundation for the research fellowship at Martin Luther University Halle-Wittenberg, Germany.

Appendix A. Supplementary data

Supplementary data to this article can be found online at <https://doi.org/10.1016/j.molliq.2020.113252>.

References

- [1] H.L. Nguyen, P.N. Horton, M.B. Hursthouse, A.C. Legon, D.W. Bruce, Halogen bonding: a new interaction for liquid crystal formation, *J. Am. Chem. Soc.* 126 (1) (2004) 16–17.
- [2] P. Metrangolo, C. Prasang, G. Resnati, R. Liantonio, A.C. Whitwood, D.W. Bruce, Fluorinated liquid crystals formed by halogen bonding, *Chem. Commun.* (2006) 3290–3292.
- [3] Prasang, H.L. Nguyen, P.N. Horton, A.C. Whitwood, D.W. Bruce, Trimeric liquid crystals assembled using both hydrogen and halogen bonding, *Chem. Commun.* (2008) 6164–6166.
- [4] M. Alaasar, S. Poppe, C. Tschierske, Photoresponsive halogen bonded polycatenar liquid crystals, *J. Mol. Liq.* 277 (2019) 233–240.
- [5] H. Wang, H.K. Bisoyi, L. Wang, A.M. Urbas, T.J. Bunning, Q. Li, Photochemically and thermally driven full-color reflection in a self organized helical superstructure enabled by a halogen-bonded chiral molecular switch, *Angew. Chem. Int. Ed.* 57 (2018) 1627–1631.
- [6] M. Saccone, L. Catalano, Halogen bonding beyond crystals in materials science, *J. Phys. Chem. B* 123 (2019) 9281–9290.
- [7] C.M. Paleos, D. Tsiourvas, Supramolecular hydrogen-bonded liquid crystals, *Liq. Cryst.* 28 (2001) 1127–1161.
- [8] T. Kato, in: D. Demus, J.W. Goodby, G.W. Gray, H.-W. Spiess, V.V. Vill (Eds.), *Handbook of Liquid Crystals*, 2B, Wiley-VCH, Weinheim 1998, p. 969.
- [9] T. Kato, T. Uryu, F. Kaneuchi, C. Jin, J.M.J. Frechet, Hydrogen-bonded liquid crystals built from hydrogen-bonding donors and acceptors infrared study on the stability of the hydrogen bond between carboxylic acid and pyridyl moieties, *Liq. Cryst.* 33 (2006) 1434–1437.
- [10] T. Kato, J.M.J. Frechet, A new approach to mesophase stabilization through hydrogen bonding molecular interactions in binary mixtures, *J. Am. Chem. Soc.* 111 (1989) 8533–8534.
- [11] U. Kumar, T. Kato, J.M.J. Frechet, Use of intermolecular hydrogen bonding for the induction of liquid crystallinity in the side chain of polysiloxanes, *J. Am. Chem. Soc.* 114 (1992) 6630–6639.
- [12] Naoum, A. Fahmi, M. Alaasar, Supramolecular hydrogen-bonded liquid crystals formed from 4-(4'-Pyridylazophenyl)-4"-substituted benzoates and 4-alkoxy benzoic acids, *Mol. Cryst. Liq. Cryst.* 482 (2008) 57–70.
- [13] H.A. Ahmed, M. Hagar, M. Alaasar, M. Naoum, Wide nematic phases induced by hydrogen-bonding, *Liq. Cryst.* 46 (2019) 550–559.
- [14] M.B. Ros Gimeno, J.L. Serrano, M.R. De la Fuente, Hydrogen-bonded banana liquid crystals, *Angew. Chem. Int. Ed.* 43 (2004) 5235–5238.
- [15] M. Gimeno, B. Ros, J.L. Serrano, Noncovalent interactions as a tool to design new bent-core liquid-crystal materials, *Chem. Mater.* 20 (2008) 1262–1271.
- [16] M. Alaasar, C. Tschierske, M. Prehm, Hydrogen-bonded supramolecular complexes formed between isophthalic acid and pyridine-based derivatives, *Liq. Cryst.* 38 (2011) 925–934.
- [17] J. Wang, Y. Shi, K. Yang, J. Wei, J. Guo, Stabilization and optical switching of liquid crystal blue phase doped with azobenzene-based bent shaped hydrogen-bonded assemblies, *RSC Adv.* 5 (2015) 67357–67364.
- [18] M.K. Paul, P. Paul, S.K. Saha, S. Choudhury, Bent shaped H-bonded mesogens derived from 1,5-bis(4-hydroxyphenyl) penta-1,4-dien-3-one: synthesis, photophysical, mesomorphism and computational studies, *J. Mol. Liq.* 197 (2014) 226–235.
- [19] B. Korkmaz, N.C. Yilmaz, Z.G. Özdemir, M. Okutan, Y.H. Gursel, A. Sarac, B.F. Senkal, Synthesis and electrical properties of hydrogen bonded liquid crystal polymer, *J. Mol. Liq.* 219 (2016) 1030–1035.
- [20] M. Pfletscher, C. Wölper, J.S. Gutmann, M. Mezger, M. Giese, A modular approach towards functional supramolecular aggregates - subtle structural differences inducing liquid crystallinity, *Chem. Commun.* 52 (2016) 8549–8552.
- [21] M. Alaasar, C. Tschierske, Nematic phases driven by hydrogen-bonding in liquid crystalline nonsymmetric dimers, *Liq. Cryst.* 46 (2019) 124–130.
- [22] R. Walker, D. Pocięcha, J.P. Abberley, A. Martinez-Felipe, D.A. Paterson, E. Forsyth, G.B. Lawrence, P.A. Henderson, J.M.D. Storey, E. Gorecka, C. Imrie, Spontaneous chirality through mixing achiral components: a twist-bend nematic phase driven by hydrogen-bonding between unlike components, *Chem. Commun.* 54 (2018) 3383–3386.
- [23] M. Alaasar, S. Poppe, Q. Dong, F. Liu, C. Tschierske, Mirror symmetry breaking in cubic phases and isotropic liquids driven by hydrogen bonding, *Chem. Commun.* 52 (2016) 13869–13872.
- [24] H. Yu Chen, M. Quan, L. Zhang, H. Yang, Y. Lu, Photothermal effect of azopyridine compounds and their applications, *RSC Adv.* 5 (2015) 4675–4680.
- [25] J. Garcia-Amorós, M. Reig, A. Cuadrado, M. Ortega, S. Nonell, D. Velasco, A photoswitchable bis-azo derivative with a high temporal resolution, *Chem. Commun.* 50 (2014) 11462–11464.
- [26] H. Yu Chen, L. Zhang, H. Yang, Y. Lu, Photoresponsive liquid crystals based on halogen bonding of azopyridines, *Chem. Commun.* 50 (2014) 9647–9649.
- [27] M. Zaremba, V. Siksnys, Molecular scissors under light control, *Proc. Natl. Acad. Sci. U. S. A.* 107 (2010) 1259–1260.
- [28] K.M. Lee, T.J. White, Photomechanical response of composite structures built from azobenzene liquid crystal polymer networks, *Polymers* 3 (2011) 1447–1457.
- [29] J. Garcia-Amorós, M. Reig, M.C.R. Castro, A. Cuadrado, M.M.M. Raposo, D. Velasco, et al., Molecular photo-oscillators based on highly accelerated heterocyclic azo dyes in nematic liquid crystals, *Chem. Commun.* 50 (2014) 6704–6706.
- [30] M. Alaasar, Azobenzene-containing bent-core liquid crystals: an overview, *Liq. Cryst.* 43 (2016) 2208–2243.
- [31] H.K. Bisoyi, Q. Li, Light-driven liquid crystalline materials: from photo-induced phase transitions and property modulations to applications, *Chem. Rev.* 116 (2016) 15089–15166.
- [32] B.N. Sunil, M.K. Srinatha, G. Shanker, G. Hegde, M. Alaasar, C. Tschierske, Effective tuning of optical storage devices using photosensitive bent-core liquid crystals, *J. Mol. Liq.* 304 (2020) 112719.
- [33] M. Hird, Fluorinated liquid crystals - properties and applications, *Chem. Soc. Rev.* 36 (2007) 2070–2095.
- [34] C. Tschierske, Fluorinated liquid crystals: design of soft nanostructures and increased complexity of self-assembly by perfluorinated segments, *Liq. Cryst.* 318 (2011) 1–108.
- [35] M. Alaasar, M. Prehm, C. Tschierske, Influence of halogen substituent on the mesomorphic properties of five-ring banana-shaped molecules with azobenzene wings, *Liq. Cryst.* 40 (2013) 656–668.
- [36] M. Saccone, K. Kuntze, Z. Ahmed, A. Siiskonen, M. Giese, A. Priimagi, Orthofluorination of azophenols increases the mesophase stability of photoresponsive hydrogen-bonded liquid crystals, *J. Mater. Chem. C* 6 (2018) 9958–9963.
- [37] M. Saccone, M. Pfletscher, E. Dautzenberg, R.Y. Dong, C.A. Michal, M. Giese, Hydrogen-bonded liquid crystals with broad-range blue phases, *J. Mater. Chem. C* 7 (2019) 3150–3153.
- [38] M. Alaasar, M. Prehm, C. Tschierske, Mirror symmetry breaking in fluorinated bent-core mesogens, *RSC Adv.* 6 (2016) 82890–82899.
- [39] M. Alaasar, M. Prehm, S. Poppe, C. Tschierske, Development of polar order by liquid-crystal self-assembly of weakly bent molecules, *Chem. -A Eur. J.* 23 (2017) 5541–5556.
- [40] M. Alaasar, M. Prehm, Y. Cao, F. Liu, C. Tschierske, Spontaneous mirror-symmetry breaking in isotropic liquid phases of photoisomerizable achiral molecules, *Angew. Chem. Int. Ed.* 128 (2016) 320–324.
- [41] X. Song, J. Li, S. Zhang, Supramolecular liquid crystals induced by intermolecular hydrogen bonding between benzoic acid and 4-(alkoxyphenylazo)pyridines, *Liq. Cryst.* 30 (2003) 331–335.
- [42] M. Spengler, R.Y. Dong, C.A. Michal, W.Y. Hamad, M.J. MacLachlan, M. Giese, Hydrogen-bonded liquid crystals in confined spaces-toward photonic hybrid materials, *Adv. Funct. Mater.* 28 (2018) 1800207–1800217.
- [43] D. Bruce, P. Metrangolo, F. Meyer, C. Präsang, G. Resnati, G. Terraneo, A. Whitwood, Mesogenic, trimeric, halogen-bonded complexes from alkoxystilbazoles and 1,4-diiodotetrafluorobenzene, *New J. Chem.* 32 (2008) 477–482.
- [44] A. Martinez-Felipe, G. Cook, J.P. Abberley, R. Walker, J.M.D. Storey, C.T. Imrie, An FT-IR spectroscopic study of the role of hydrogen bonding in the formation of liquid crystallinity for mixtures containing bipyridines and 4-pentoxibenzoic acid, *RSC Adv.* 6 (2016) 108164–108179.
- [45] Y. Arakawa, Y. Sasaki, K. Igawa, H. Tsuji, Hydrogen bonding liquid crystalline benzoic acids with alkylthio groups: phase transition behavior and insights into the cybotactic nematic phase, *New J. Chem.* 41 (2017) 6514–6522.
- [46] G.W. Gray, J.W. Goodby, *Smectic Liquid Crystals*, Leonard Hill, Glasgow, 1984.